Hindawi
Advances in Materials Science and Engineering
Volume 2018, Article ID 8106189, 14 pages
https://doi.org/10.1155/2018/8106189

Research Article

A Novel and Facile Nanoclay Aerogel Masterbatch toward Exfoliated Polymer-Clay Nanocomposites through a Melt-Mixing Process

Wasuthep Luecha[1,2] **and Rathanawan Magaraphan**[1,2,3]

[1]*Polymer Processing and Polymer Nanomaterials Research Unit, Chulalongkorn University, Bangkok 10330, Thailand*
[2]*The Petroleum and Petrochemical College, Chulalongkorn University, Bangkok 10330, Thailand*
[3]*Green Materials for Industrial Application Research Unit, Faculty of Science, Chulalongkorn University, Bangkok 10330, Thailand*

Correspondence should be addressed to Rathanawan Magaraphan; rathanawan.k@chula.ac.th

Received 1 May 2018; Accepted 26 June 2018; Published 2 August 2018

Academic Editor: Mohammad Luqman

This research employed a novel and facile approach called nanoclay aerogel masterbatch.. This innovative technique was conducted by attaching the clay layers directly onto a mobile polymer, for example, polyethylene glycol (PEG), in order to modify the clay layer through PEG-clay intercalation and PEG-hydrogen bonding. This state was maintained with a small amount of the anionic polymer hydrogel, for example, kappa-carrageenan (KC), and turning it into a highly porous and fragile structure by freeze-drying, thus a so-called nanoclay aerogel masterbatch. The facile nanoclay aerogel masterbatch was able to be attained even at high clay loadings (55–67 wt.% of the inorganic clay content) with constant PEG and KC loadings. The interlayer spacing enlargement of the nanoclay galleries was around 17 Å with the typical lamellar morphology like a house of cards structure. The density values were within 0.108–0.122 g·cm^{-3}. The thermal stabilities were up to 270°C, revealing better thermal stability for melt mixing with the commodity plastics at a high melting temperature. The flowability and processability were certified by the melt flow index (MFI) results. The highest nanoclay loading capacity (67 wt.%) of the achieved nanoclay aerogel masterbatch was selected to prepare PS-clay nanocomposites via a melt-mixing process. The comparative nanocomposites were produced by using organoclay. The results of the X-ray diffraction (XRD) and transmission electron microscopy (TEM) exhibited that the exfoliated morphologies were obtained at all clay contents (1–3 wt.%); however, the intercalated structure was gained by using organoclay. The outstanding transparency and brightness were remarked from the specimens prepared by using the nanoclay aerogel masterbatch. The brownish specimens were observed by using organoclay. The significant improvements of tensile properties, glass transition temperature (T_g), and thermal stability were noticed from the nanocomposites prepared using the nanoclay aerogel masterbatch.

1. Introduction

Polymer nanocomposites based on nanoclays have received much interest due to the superior improvements of the mechanical, thermal, barrier, and flame-retardant properties [1, 2]. The natural nanoclays are hydrophilic which is a problem for homogeneous dispersion in several polymers, so the nanoclays have to be developed to be an organoclay through the alkylammonium cation-exchange method [3, 4]. There are many disadvantages of organoclay, such as the expensive cost of organoclay due to the use of an excessive amount of the expensive surfactant to ensure complete ion exchange, the high energy consumption of the entire organoclay preparation, the tendency of particle agglomeration, and unexpected poor dispersion in the polymer matrix. The key to the property enhancement of polymer-clay nanocomposites is to accomplish exfoliated layered silicate with homogeneous dispersion in the polymer matrix

[1–3, 5–22]. A hot-melt extrusion process has been widely used to prepare polymer-clay nanocomposites in the industrial production because it is simple and environmentally friendly [17]. During the melt blending at a high shear rate, the polymer chains of the molten polymer penetrate into the nanoclay galleries to achieve either intercalated or exfoliated nanocomposite structures depending on the degree of penetration [23]. A nanoclay masterbatch is a technique that incorporates a high percentage of nanoclay loading in a carrier polymer before being diluted by blending with a raw polymer to permit better nanoparticle dispersion [3, 14]. The benefits of this technique are the exact defined nanoclay quantity without any handling of large powder masses. Therefore, the environment is not damaged by the pollution of spreading nanoclay dust. A number of previous research studies have reported that the nanocomposites prepared from melt mixing seemed to only have success with partially exfoliated morphologies [2, 10, 12, 16, 17, 20, 23–27].

The novel nanoclay masterbatch was potentially fabricated through a new approach initially represented as "nanoclay gel" and eventually transferred to a "nanoclay aerogel masterbatch." This innovative strategy started from the expansion property of the layered silicates in an aqueous solution due to the repulsive force of the negative charges on the surface of the layered silicate sheets [28]. In the swollen state of layered silicate clays, the nonionic water-soluble polymer having a higher molecular weight and more thermal stability than quaternary ammonium salts was used for both the intercalation and surface modification of the layered silicates. Emphasis was given to polyethylene glycol (PEG) because it should be water soluble, have a high degree of organophilicity, and not have a high molecular weight to allow good flowing ability [15]. Moreover, PEG-treated nanoclay is thermally stable at 327°C in an inert atmosphere and 275°C in air, which is greater than alkylammonium salts; therefore, it could be processed at a higher temperature without thermal degradation than typical organoclay [17, 29]. According to the reports of Zampori et al. [30], Finocchio et al. [31], and Belova et al. [32], PEG with the MW of 1500 (PEG1500) was used as a nonionic surfactant to prepare the organoclays. The PEG-intercalated clay had the ability to modify the clay's surface to be organophilic due to the interaction between the oxygen atoms of the PEG molecule and sodium cations dwelling in the interlayers of the layered silicate and between the PEG molecule and nanoclay surface via hydrogen bonding; hence, the long tails of the PEG molecular chain were able to interact with the organic polymer [12, 15, 33, 34]. This process was similar to the conventional preparation of organoclay using small molecules of polar polymers instead of the general surfactant. PEG functioned by improving the processability with the provision of the homogeneous dispersion of the nanoclay in the polymer matrix through melt mixing [35, 36]. A solution of the polymer-intercalated clay nanocomposite was accomplished. Instead of following the process by evaporation and grinding into clay powder, the clay/polymer intercalation solution was turned into gel with a small amount of hydrogel and sustained in the gel form. A negatively charged hydrogel was favorably selected in order to preserve the interlayer-expanded structure. This polymer/clay nanocomposite hydrogel was sustained and represented as a "nanoclay gel." The property of the hydrogel that was selected to maintain the swollen state of the clay/PEG intercalation was a thermolytic hydrogel type with a physical gelation (no rigid network formation). Kappa-carrageenan (KC) is a natural hydrocolloid containing one sulphate group per disaccharide. KC is capable of forming thermoreversible gel with gelation upon cooling and melting upon heating [37]. Moreover, KC exhibits a negative charge when dissolved in water; thus, the negatively charged system benefits to preserve the extended clay galleries (swollen state) of the PEG-intercalated nanoclay during the transformation from a dispersed liquid to gel without penetrating the KC chains into a layered silicate spacing [38]. Minimal KC concentration of 1 wt.% was reported to create sufficient gelation on cooling [39–41]. With regard to the reduction of the expansion of the nanoclay galleries and the strong stacking of nanoclay when the water was gradually evaporated during the hot-drying stage, freeze-drying was proposed to prepare the facile "nanoclay aerogel masterbatch" instead of conventional hot drying. Aerogel is a porous solid material created in the form of an interconnected three-dimensional network structure with a high specific surface area, high porosity, and low density [42, 43].

It should be noted that the nanoclay aerogel can be used as a masterbatch to prepare a polymer-clay nanocomposite via a melt extrusion process. The fragile and porous structure of nanoclay aerogel benefits the good dispersion of the nanoclay particle in the polymer matrix and further achieves the exfoliated morphology [44]. The expected advantages of this nanoclay aerogel masterbatch were probably the outcome of the lean manufacturing for polymer-clay nanocomposite industries besides having nanoclay loading, for example, easy manipulation than fine powder, extraordinary nanoclay-loading capacity, economical material and production costs, zero waste, environmentally friendly production process, and the ability for organophilic modification without using an expensive cationic surfactant.

The facile nanoclay aerogel masterbatches were fabricated with a variation of high nanoclay-loading capacities and steady contents of PEG and KC. The nanoclay gels were subsequently turned into nanoclay aerogels via a freeze-drying process. The success of this strategy to obtain exfoliated morphologies and a nanocomposite with property enhancement was demonstrated by using the nanoclay aerogel masterbatches to prepare polystyrene- (PS-) clay nanocomposites compared to the conventional nanocomposites of PS-organoclay.

2. Materials and Methods

2.1. Materials. Na^+-bentonite clay (Ben, grade SAC) was obtained from the Thai Nippon Chemical Industry Company Limited with a cation-exchange capacity (CEC) of 75 meq/100 g. Commercial kappa-carrageenan (KC) was provided by the Ingradianflewer Company Limited. Commercial polyethylene glycol (PEG 1450) was supplied by the Dow Chemical Company. Hexadecyltrimethylammonium

chloride ($C_{19}H_{42}N^+Cl^-$) used as a cationic surfactant for the organoclay preparation was obtained from Evonik Industries. Polystyrene (PS, Styron 656D) with a density of 1.04 g/cm^{3}and an MFI of 8.5 g/10 min was supplied by the Dow Chemical Company, Thailand. Deionized water (DI) was applied throughout the whole work.

2.2. Preparation of the Nanoclay Gel. The compositions used to prepare the nanoclay gels are shown in Table 1. Initially, the variations of the nanoclay suspensions were produced by swelling 10, 20, and 30 g of nanoclay powder in 200 cm^3 of DI water and stirred by means of a mechanical stirrer for 24 hours at room temperature (28°C). In this study, the composition of PEG was kept constant at 10 g for all nanoclay suspensions, and the desired KC concentration of the final mixtures was fixed at 1% w/v because this was the minimum concentration to form gel on cooling. Then, the nanoclay/PEG mixtures were prepared by mixing between the desired nanoclay suspension and PEG and continuously sheared by using the mechanical stirrer (running at 1000 rpm) for 90 minutes while the temperature was controlled at 60°C. The 3% w/v of the KC solution was prepared separately by dissolving 3 g of KC powder in 100 cm^3 of DI water at 90°C under magnetic stirring until the KC was completely dissolved. Then, the KC solution was poured into the nanoclay/PEG mixtures and consistently stirred at 60°C for 15 minutes. The final concentration of KC in the mixtures was achieved at 1% (w/v). The nanoclay/PEG/KC mixtures were increasingly homogenized by using a high-speed homogenizer (Polytron PT3100) at 20,000 rpm for 15 minutes in order to ensure the homogeneous dispersion of the highly concentrated mixtures and aid the expansion of the clay galleries. The mixtures were left to cool down to room temperature and poured into cylindrical polystyrene vials. The nanoclay/PEG/KC mixtures were transformed into a gel by cooling at 10°C for 12 hours in order to maintain the swollen state of the interlayer spacing of the nanoclay platelets. All accomplished samples were denoted as nanoclay gels.

2.3. Preparation of the Nanoclay Aerogel Masterbatch. The nanoclay gels were placed in a freezer at −80°C for 24 hours. The frozen samples were then attached to a freeze-dryer (ScanVac CoolSafe) and maintained at −110°C in a vacuum of less than 400 m Torr for 72 hours to entirely sublime the solid ice into a vapor state. The inorganic clay content was examined by calculating the residual remaining at 800°C under a nitrogen atmosphere by using a simultaneous thermal analyzer (NETZSCH, STA 449 F3) from 30 to 800°C with a heating rate of 10°C·min^{-1} under an oxygen atmosphere with a flow rate of 30 ml/min. As shown in Table 1 and Figure 1, the pristine nanoclay aerogel prepared using 10 g of nanoclay powder swollen in 200 cm^3 of DI water was labelled as pure nanoclay aerogel, and the nanoclay aerogel masterbatches prepared from 10, 20, and 30 g of nanoclay powder with the fixed compositions of PEG and KC were coded as Aerogel_55, Aerogel_61, and Aerogel_67, respectively, that corresponded to the inorganic clay contents.

2.4. Preparation of the Organoclay. The organoclay was obtained by the modification of bentonite with hexadecyltrimethylammonium chloride ($C_{19}H_{42}N^+Cl^-$) via a cation-exchange method, represented as "ORG." The inorganic content of the organoclay was 79.1 wt.%.

2.5. Preparation of the Polymer/Clay Nanocomposites

2.5.1. The Melt Extrusion Process. The melt blending of PS and nanoclay aerogel masterbatch (Aerogel_67) was conducted in a corotating twin screw extruder (Labtech Engineering company; L/D ratio of 40 : 1). Initially, pure PS was dried at 80°C under a vacuum for 12 hours. The PS was mixed with 1, 2, and 3 wt.% of inorganic clay contents by stoichiometric calculation. 98.5, 97.0, and 95.5 g of PS were combined with actual loadings of the nanoclay aerogel masterbatch of 1.5, 3.0, and 4.5 g in order to produce the PS/clay nanocomposite containing 1, 2, and 3 wt.% of inorganic clay contents, denoted as PS/Aero-1, PS/Aero-2, and PS/Aero-3, respectively. The PS/clay nanocomposites produced from organoclay were simultaneously prepared in order to compare the nanocomposite properties. 98.7, 97.5, and 96.2 g of pure PS were mixed with 1.3, 2.5, and 3.8 g of actual organoclay amounts to create the PS/clay nanocomposites having 1, 2, and 3 wt.% of inorganic clay contents, which were coded as PS/ORG-1, PS/ORG-2, and PS/ORG-3, respectively. The extruded strands were pulled through a water bath at 20°C and cut into pellets using a pelletizer and an air knife. The temperature profiles of the extrusion process ranged from 180°C in the feed zone to 200°C in the die zone, and the screw speed was set as 70 rpm.

2.5.2. Specimen Preparation. The pellets of the PS/clay nanocomposites were injected as per ASTM D638 using an injection molding machine (Elite 80) into a dog-bone shape at the temperature range of 190–210°C.

2.6. Characterizations

2.6.1. The X-Ray Diffraction (XRD). The XRD analysis of the nanoclay aerogel masterbatches, organoclay, and PS/clay nanocomposites was carried out to investigate the basal spacing (d_{001} spacing) of the silicate interlayers. The measurements were conducted by using a Bruker AXS X-ray diffractometer with CuK radiation ($\lambda = 1.54056$ Å). The generator was performed at 40 kV and 40 mA. The spectra were recorded over a 2θ range of 2–10° using a scan rate of 0.01°/s.

2.6.2. Scanning Electron Microscope (SEM). The morphology of the cross-sectional surface was determined using a scanning electron microscope (JEOL, model JSM 5200). The nanoclay aerogel masterbatches were prepared by fracturing small pieces of the monolithic nanoclay aerogel masterbatches

Table 1: Nanoclay aerogel masterbatch compositions.

Nanoclay aerogel masterbatch samples	Nanoclay gel				Nanoclay aerogel masterbatch (inorganic clay content)* (%)
	Ben (g)	KC (g)	PEG (g)	Water content (cm^3)	
Pure nanoclay aerogel	10	—	—	200	86
Aerogel_55	10	3	10	300	55
Aerogel_61	20	3	10	300	61
Aerogel_67	30	3	10	300	67

*From TGA results of the residual remaining at 800°C under a nitrogen atmosphere.

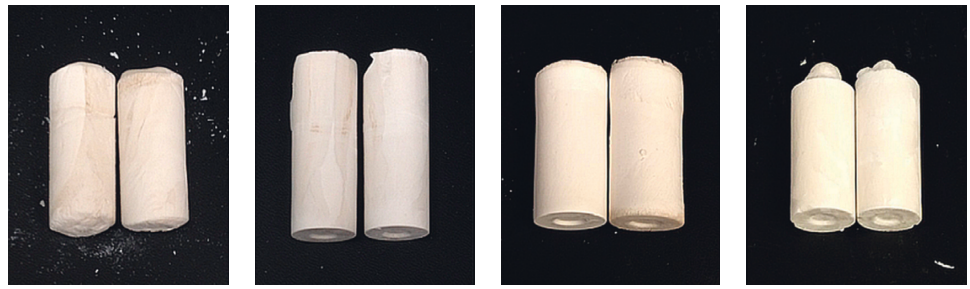

(a) (b) (c) (d)

Figure 1: Photographs of cylindrical aerogels: (a) pure nanoclay aerogel; (b) Aerogel_55; (c) Aerogel_61; (d) Aerogel_67.

in order to investigate the internal morphology of these aerogel samples. The PS/clay nanocomposite specimens were fractured in liquid nitrogen. Subsequently, the samples were coated with gold under a vacuum using JFC-1600 (JEOL) sputtering before imaging in order to increase the image resolution. All SEM images were taken at an acceleration voltage of 5.0 keV.

2.6.3. Density. The density of the nanoclay aerogel masterbatches was calculated by dividing the dry mass of the nanoclay aerogels by the volume. The volume was measured by a digital caliper. The mass was measured by an analytical balance with 4-digit sensitivity. The density values were calculated from the average of 5 samples for each condition set.

2.6.4. Melt Flow Index (MFI). The MFI of the nanoclay aerogel masterbatches was calculated by a melt flow index tester (Dynisco) according to the ASTM standard D1238-04. The melting temperature was kept at a uniform 200°C, with a 5.0 kg load adapted to extrude in a molten state by setting up the cutoff times for 10 seconds. A 100 g rod was used as a plunger, and the molten material flowed through an orifice of 2.0 mm diameter. The average MFI values were calculated from five calculations.

2.6.5. Thermal Stability. The thermal stability of the nanoclay aerogel masterbatches and PS/clay nanocomposite samples was characterized by a simultaneous thermal analyzer (NETZSCH, STA 449 F3) with the heating rate of 10°C/minutes from 30°C to 800°C under a nitrogen atmosphere with a flow rate of 30 ml/minute. The percentage of the weight loss was reported as a function of the temperature.

2.6.6. Thermal Behavior. The thermal behavior of the PS/clay nanocomposite samples was investigated by using differential scanning calorimetry (DSC) with a Mettler Toledo model DSC822 working on a Pyris platform under a nitrogen atmosphere to avoid any possible thermal degradation. The weight of the samples was in the range of 5–10 mg. The thermal scan was the first heating cycle from 25°C up to 200°C, held at 200°C for 3 minutes, and then cooled to 25°C at the constant rate of 10°C/minute. The glass transition temperature (T_g) was recorded during a second heating cycle.

2.6.7. Transmission Electron Microscopy (TEM). The morphology of the PS/clay nanocomposite samples was observed using transmission electron microscopy (TEM). Firstly, the nanocomposite samples were prepared by cutting thin (~200 nm) slices of the samples, precut into a pyramid-shaped point, and then ultramicrotomed at room temperature, with the sections placed onto porous carbon film-coated TEM grids. The samples were embedded in a TEM-grade epoxy and then precut and ultramicrotomed at room temperature. Once on the TEM grids, the PS/clay nanocomposite samples were loaded into a liquid-nitrogen-cooled cryogenic TEM holder and imaged in the TEM with the samples maintained at a temperature of −60°C to prevent the samples from burning in the TEM. The ultramicrotome used was a Leica model Ultracut UCT with a cryoattachment EM-FCS with diamond knives used for both room temperature and cryogenic cutting. The TEM was a JEM-2100 microscope, operated at 200 keV

with an LaB_6 filament; the digital images were recorded on a 1×1K digital camera attached to the GIF (Gatan image filter). The cryoholder was a Gatan model 613 cold stage with a Smart set temperature controller.

2.6.8. Tensile Testing. The tensile properties such as tensile strength, elongation at the break, and Young's modulus of the PS/clay nanocomposite samples were examined using a universal testing machine (Instron:H10KM) according to ASTM D638-08. The tensile tests were conducted at room temperature, and the crosshead speed was set at 10 mm/minute. The average values were reported from at least five specimens for each set of conditions.

3. Results and Discussion

3.1. Part 1: Preparation of the Nanoclay Aerogel Masterbatch. The basal spacing of the nanoclay (d_{001}) investigated using XRD in the range of $2\theta = 2$–10° is reported in Table 2 and Figure 2. The pure nanoclay powder showed the diffraction peak at $2\theta = 7.33^\circ$ with the spacing of 12.05 Å. The pure nanoclay aerogel revealed an indifferent change compared to the nanoclay powder in the diffraction peaks (at $2\theta = 6.97^\circ$) and d_{001} spacing (12.68 Å). This result suggested that the interlayer spacing was not compressed by the pressure generated from the expansion of the ice crystal. Due to the XRD results of the nanoclay aerogel masterbatches compared to pure nanoclay aerogel, the obvious shifts of the d_{001} reflections to lower 2θ positions (at 5.14–5.19°) were clearly observed corresponding to the significant increases of basal spacing (17.04–17.09 Å). These results confirmed the intercalation of the PEG molecules inside the interlayer spacing of the nanoclay forming the bilayer arrangement of the PEG chains laying parallel into the silicate interlayers [45]. This similarity was reported by Alhassan et al. [46]. It could be attributed that intercalation had taken place during the preparation of the nanoclay gel from the driving force of the water-swollen clay, which generated the positive entropy [47–49]. Moreover, the enthalpic driving force occurred from the interactions from the hydrogen bonding between the hydroxyl and ether oxygen groups of PEG, water molecules, and Si-O-Si on the clay surfaces [12, 50]. Numerous studies have reported similar results based on the intercalated PEG/clay nanocomposites, such as Zampori et al. [30], Finocchio et al. [31], Clegg et al. [50], and Campbell et al. [36]. This result could be attributed to the organophilicity of the achieved nanoclay aerogel masterbatches, which was enhanced from this process that resembled the typical surface modification of the organoclay preparation. Upon addition of the nanoclay loadings from 55 to 67 wt.%, the d_{001} spacing slightly decreased by the d-values 17.18, 17.09, and 17.04 Å of Aerogel_55, Aerogel_61, and Aerogel_67, respectively. This result may be ascribed due to the limitation of the expanded space with a greater occupied volume of a higher clay content. According to the XRD results, it should be noted that the enlargement of the intercalation degree had a tiny effect from the increment of the nanoclay content. In summary, the expansion of the clay galleries with the intercalated PEG chains (d-value 17.04–17.18 Å) was a success with the high clay loadings (55–67 wt.%).

Table 2: Basal spacing of nanoclay aerogel masterbatches.

Sample	2θ (°)	d_{001} (Å)
Pure nanoclay powder	7.33	12.05
Pure nanoclay aerogel	6.97	12.68
Aerogel_55	5.14	17.18
Aerogel_61	5.17	17.09
Aerogel_67	5.19	17.04

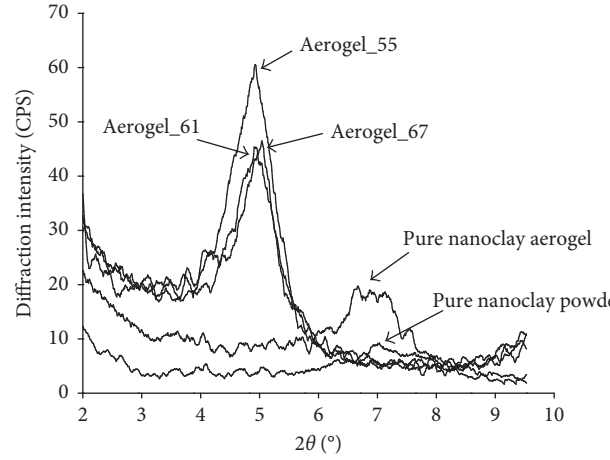

Figure 2: XRD patterns of nanoclay aerogel masterbatches.

Figure 3 illustrates the samples of the achieved nanoclay aerogel masterbatch that was started from the homogeneous nanoclay solution. By adding a small amount of carrageenan, it was changed into a gel in order to preserve the swelling state of the intercalated PEG-clay nanocomposites. Finally, the nanoclay gel samples were turned into aerogel through a freeze-drying process in order to maintain the expansion of the expanded clay galleries without the collapse or reduction of the layered silicate enlargement when the water content was gradually evaporated. It should be noted that this method had a noticeable advantage of not only having an easier preparation with the intercalation and organoclay modification occurring in one step but also having more economical preparation with inexpensive ingredients than the conventional organoclay preparation.

The nanoclay aerogel masterbatch morphology was imaged by scanning electron microscopy (SEM) and is shown in Figure 4. It was evident that all of the nanoclay aerogel masterbatches exhibited a typical lamellar morphology, which is also known as the house of cards structure that was created from the ice crystal growth via a freeze-drying process [51, 52]. The lamellar structures and voids inside the nanoclay aerogel structures were created by the sublimation of ice. Similar results were reported in many studies based on preparing polymer/clay aerogels with various types of polymers [42, 51–58]. The denser lamellar morphology was observed with the increase of the nanoclay loadings due to the limitation of the expanded space between the adjacent lamellar at a high nanoclay content. Noticeably,

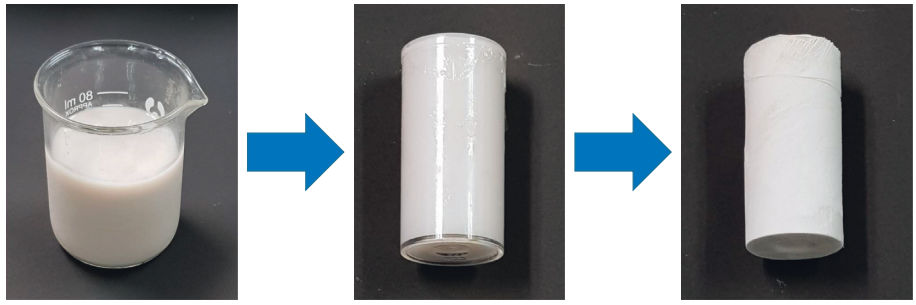

Figure 3: The illustration steps of nanoclay aerogel masterbatch preparation.

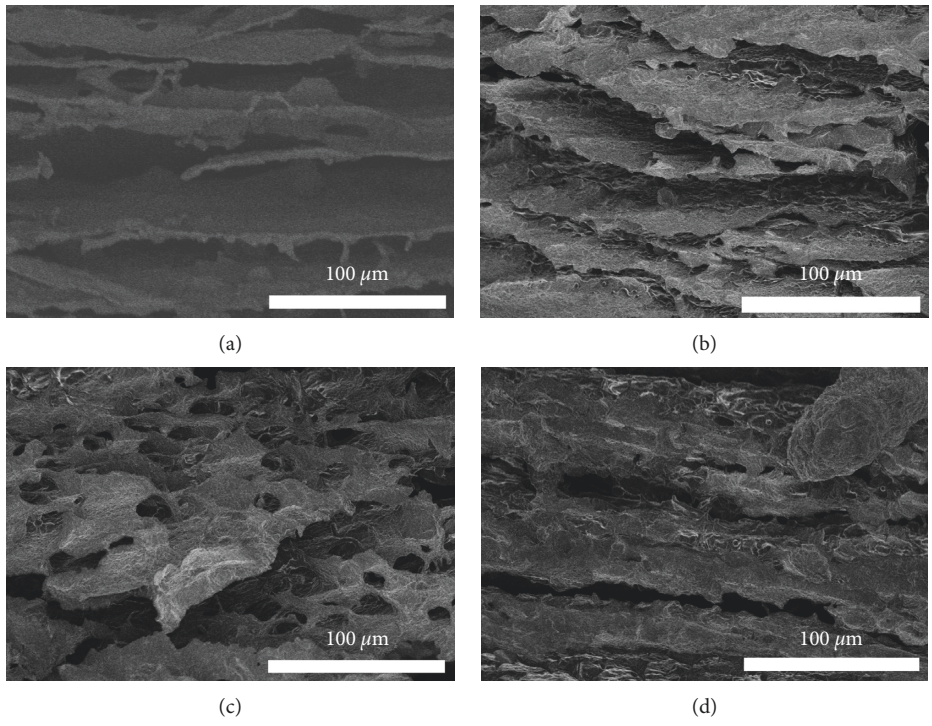

Figure 4: SEM images of nanoclay aerogel masterbatches: (a) pure nanoclay aerogel; (b) Aerogel_55; (c) Aerogel_61; (d) Aerogel_67.

Table 3: Density and MFI results of nanoclay aerogel masterbatches.

Sample	Density ($g \cdot cm^{-3}$)	MFI (g/10 min; 200°C, 5.0 kg load)
Pure nanoclay aerogel	0.082 ± 0.002	—
Aerogel_55	0.108 ± 0.006	0.55 ± 0.04
Aerogel_61	0.115 ± 0.003	0.51 ± 0.04
Aerogel_67	0.122 ± 0.004	0.48 ± 0.02

the porous structure of the house of cards observed from the achieved nanoclay aerogel masterbatches contained a high nanoclay loading (55–67 wt.%). It was anticipated that this fragile porous structure would facilitate the layer dispersion to enhance the opportunities for exfoliation.

From Table 3, the nanoclay aerogels had density values within 0.11–0.12 $g \cdot cm^{-3}$. In other words, the density increased by 32, 40, and 49% for the inorganic clay content of 55, 61, and 67 wt.%, respectively, compared to the pristine nanoclay aerogel. It was noticed that the density values of the nanoclay aerogels rose with the increased nanoclay loading due to the high density of the rigid clay particles. This result supported the dense morphology with a high nanoclay content.

The flowability and processability of the nanoclay aerogel masterbatch for melt mixing were investigated by MFI. The MFI of the nanoclay aerogel masterbatch was calculated at the temperature of 200°C under a 5.0 kg load. The MFI values diminished from 0.55 to 0.48 g/10 minutes by increasing the nanoclay loading ascribed to increasing the viscosity (as shown in Table 3). Moreover, the continuous smooth surface of the extrudates was observed with no significant change in the color through the simple melt extruded simulation. The MFI results suggested that the achieved nanoclay aerogel

masterbatches were composed of flowable and processable properties; therefore, they had the capability to attain good dispersion and exfoliated potential.

The thermal degradation temperature of the nanoclay aerogel masterbatch is very important to consider for the melt extrusion process in order to ensure that there is no thermal decomposition occurring during the melt blending process. The upper processing temperature was characterized by thermogravimetric analysis. The onset decomposition temperature ($T_{d,onset}$), the maximum decomposition rate temperature ($T_{d,max}$), and residual weight at 800°C of the nanoclay aerogel masterbatches are exhibited in Table 4 and Figure 5. The results revealed the starting of thermal degradation at a minimum of 258°C to a maximum of 270°C; the maximum thermal decompositions were reported from the minimum of 336°C to a maximum of 340°C. The improvement of thermal stability ($T_{d,onset}$ and $T_{d,max}$) was observed by increasing the added nanoclay content due to the rigid nanoclay particles that acted as a physical barrier to improve the thermal resistance of the achieved nanoclay aerogels [13, 58, 59]. It should be noted that the accomplished nanoclay aerogel masterbatches could safely melt since the beginning of their decomposition temperatures was higher than the processing temperatures of the commodity plastics [60].

3.2. Part 2: Preparation of the PS/Clay Nanocomposite via the Melt Extrusion Process. In Part 2, Aerogel_67 that contained a higher nanoclay content was selected to use as a nanoclay masterbatch to be melted compounded with polystyrene to prepare the PS/clay nanocomposites having 1, 2, and 3 wt.% of the inorganic clay contents, referred to as PS/Aero-1, PS/Aero-2, and PS/Aero-3, respectively. For comparison, the PS/organoclay nanocomposites were prepared by using organoclay (ORG) with the same contents of inorganic nanoclay (represented as PS/ORG-1, PS/ORG-2, and PS/ORG-3, resp.). The dispersion of the nanoclay particles was examined by XRD and TEM. Meanwhile, the mechanical and thermal properties were characterized by tensile testing, DSC, and TGA.

As reported by the previous research, the morphology of the PS-clay nanocomposites prepared by the melt extrusion process was achieved mostly as intercalated structures; exfoliation was very difficult to attain success [61]. The XRD patterns of PS/Aero and PS/ORG are illustrated in Figure 6. The exfoliated nanocomposite structures were obtained from all loadings of PS/Aero due to the absence of the diffraction peaks from 2 to 10 Å of the diffraction angle, as represented in Figure 6(a). Meanwhile, the morphological structures obtained from PS/ORG were of intercalated type with a high d-spacing of 35.75, 35.55, and 33.31 Å for 1, 2, and 3 wt.% loadings, compared to the original d-spacing of ORG (27.97 Å) exhibiting the intercalation of the PS molecular chains inside the clay galleries, as shown in Figure 6(b). This result clearly indicates that a simple ORG with an intermediate d-spacing about 28 Å could only generate an intercalated nanocomposite structure. On the contrary, the nanoclay aerogel masterbatch with a low d-spacing of 17 Å successfully provided the exfoliated nanocomposites prepared via melt extrusion up to 3 wt.%.

Corresponding to the XRD results as shown in Figure 7, the TEM image of PS/Aero-3 exhibited the exfoliated structure with the dark lines of the individual clay sheets distributed in the polymer matrix. However, the PS/ORG-3 nanocomposite clearly illustrated the intercalated structure with stacks of clay layers. The XRD and TEM results clearly supported the hypothesis that the nanoclay aerogel masterbatches were further effective to achieve the exfoliated structure through the melt-mixing process. This accomplishment suggested that the fragile and porous structure of the nanoclay aerogel would be useful as an efficient precursor to obtain the exfoliated morphology. Furthermore, nanoclay aerogel masterbatches modified with PEG facilitated the exfoliated nanocomposites of layered silicates. PEG played a key role in intercalated PEG/nanoclay with higher expansion of basal spacing, resulting in the reduction of Van der Waals attractive forces of layered clay sheets [62]. The melted polymer chains with high shearing in the internal mixer could be able to penetrate into the expanded gallery space in order to delaminate the clay pellets during the melt-compounding process [63]. In addition, PEG acted as the dispersing agent to improve the dispersion of nanoclay particles within the polymer matrix.

Therefore, the XRD and TEM results suggested that there was powerful interfacial adhesion between the individual nanoclay particles and PS matrix [64]. This effect caused significant improvement of the tensile properties in the exfoliated morphology but no extraordinary enhancement for the intercalation of the nanocomposite structures due to the stronger interaction between the PS matrix and nanoclay particles as well as the higher aspect ratio of the filler affecting the significant enhancement of the tensile properties [13, 61, 64].

The photographs that expressed the transparency of the PS/Aero and PS/ORG nanocomposites are shown in Figure 8. The outstanding transparency and brightness were remarkable for PS/Aero-1. The gradual color change was revealed in the PS/Aero samples by increasing the nanoclay aerogel masterbatch loading. It might be ascribed that this existence resulted from the good dispersion of the individually exfoliated nanoclay particles. The presence of dark-brownish PS/ORG specimens indicated the degradation of the organic surfactant at the processing temperature [13]. In other words, the light color of PS/Aero was due to the good thermal stability of the nanoclay aerogel masterbatches.

Young's modulus of PS-clay nanocomposites was considerably improved by increasing the clay loadings from 1 to 3 wt.%, as illustrated in Table 5. These results were described by the high performance of the nanoclay particles to resist the plastic deformation, and the rigidity of the nanoclay improved the stretching resistance [65]. In particular, Young's modulus values of the PS/Aero nanocomposites (increasing by about 10%, 14%, and 19% of PS/Aero-1, PS/Aero-2, and PS/Aero-3, resp., compared to the pristine PS) were higher than the PS/ORG nanocomposites (increasing by about 8%, 11%, and 17% of PS/ORG-1, PS/ORG-2, and PS/ORG-3, resp.). It should

Table 4: TGA results of nanoclay aerogel masterbatches.

Nanoclay gel samples	$T_{d,onset}$ (°C)	$T_{d,max}$ (°C)	Residual mass (%)
Pure nanoclay aerogel	611	659	86
Aerogel_55	258	336	55
Aerogel_61	267	336	61
Aerogel_67	270	340	67

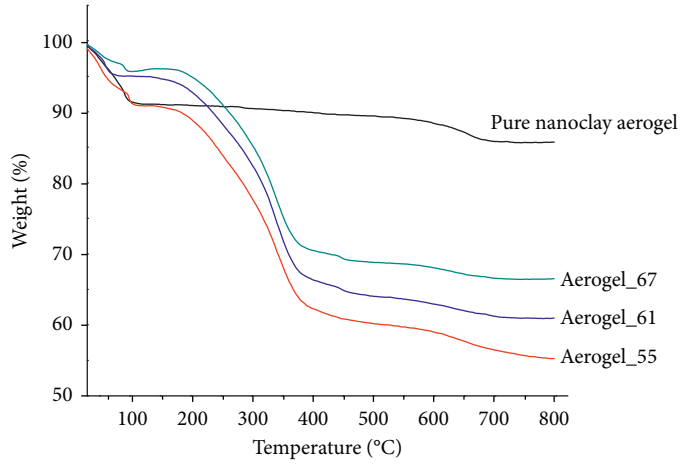

Figure 5: TGA thermogram of nanoclay aerogel masterbatches.

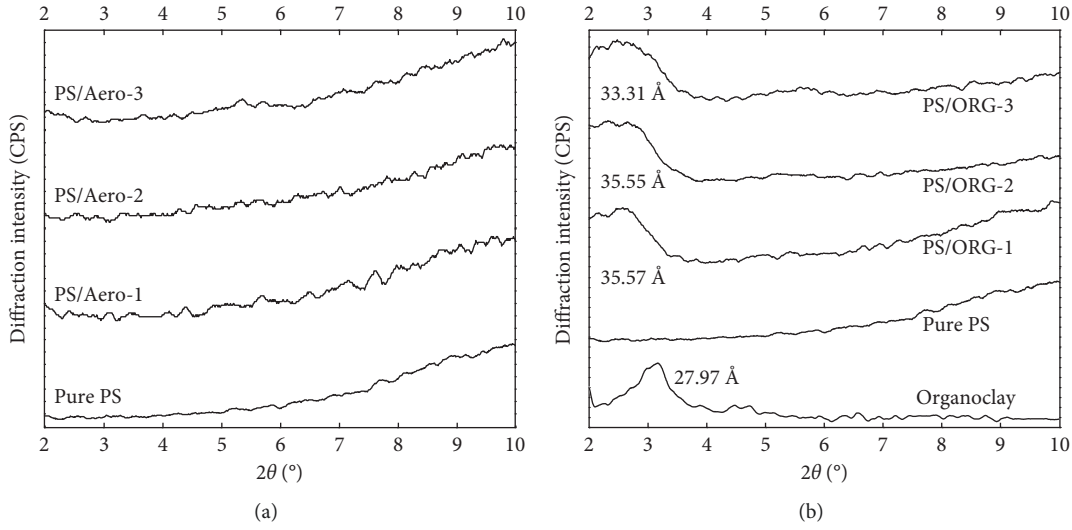

Figure 6: XRD patterns of PS/clay nanocomposites prepared from the nanoclay aerogel masterbatch and organoclay.

be anticipated that the results were due to the exfoliated nanocomposite structures. The improvement of the modulus intensively relates to the volume of the filled clay as well as the strong interaction between the nanoclay particles and polymer matrix [21]. On the contrary, the low aspect ratio of the intercalated clay stacks, as presented in PS/clay nanocomposites prepared by the organoclay, affected the weak interaction [13]. Similar results were reported from the previous studies of Uthirakumar et al. [64] and Mohanty and Nayak [65].

According to Table 5, the tensile strength of PS/Aero was progressively developed by increasing the clay loadings from 1 to 3 wt.% with improvement of about 30–33% compared to that of pristine PS due to the exfoliated structure [13, 61]. This result reveals the powerful interfacial adhesion between the individual nanoclay particles and PS matrix as a result of the clay exfoliation, which was verified by the XRD and TEM results [64]. These outcomes corresponded with the research of Uthirakumar et al. [64], Mohanty and Nayak [65], and Park et al. [22]. The tensile strength of PS/ORG was highly enhanced at a low nanoclay loading of 1 wt.% improving by about 15% compared to the pristine PS and continuously decreased from 9% to 3% enhancement with the increment of the nanoclay contents from 2 to 3 wt.%, respectively. This revealed that as the ORG loading increased, PS/ORG became

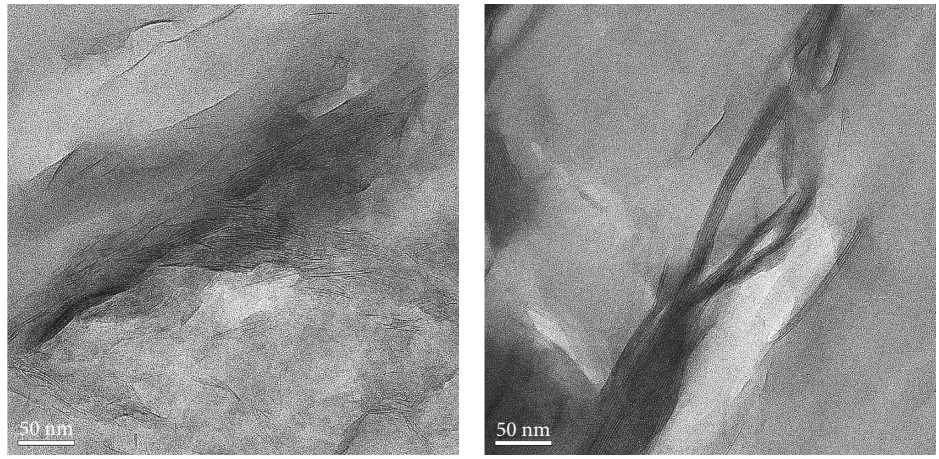

(a) (b)

Figure 7: TEM micrographs of PS/clay nanocomposites prepared from the nanoclay aerogel masterbatch and organoclay (at 3 wt.% clay loading). (a) PS/Aero-3. (b) PS/ORG-3.

Figure 8: Transparency images of PS/clay nanocomposites prepared from the nanoclay aerogel masterbatch and organoclay.

Table 5: Tensile properties of PS/clay nanocomposites prepared from the nanoclay aerogel masterbatch and organoclay.

Sample	Young's modulus (MPa)	Tensile strength (MPa)	Elongation at break (%)
Pure PS	1241 ± 15	33 ± 4	3.8 ± 0.4
PS/Aero-1	1365 ± 16	43 ± 1	3.8 ± 0.1
PS/Aero-2	1411 ± 19	43 ± 1	3.7 ± 0.1
PS/Aero-3	1481 ± 14	44 ± 1	3.7 ± 0.1
PS/ORG-1	1339 ± 20	38 ± 3	3.1 ± 0.3
PS/ORG-2	1379 ± 14	36 ± 2	2.9 ± 0.2
PS/ORG-3	1446 ± 23	34 ± 3	2.7 ± 0.3

a less intercalated clay structure with the decrease of expanded clay galleries suggesting the lack of strong polymer-filler interaction resulting in the reduction of the cohesive forces inside the materials [61, 66].

The elongation at the break of PS/Aero and PS/ORG decreased with the increase from 1 to 3 wt.% of the clay contents, as exhibited in Table 5 and Figure 9. Similar results were reported from many prior studies of PS/clay nanocomposites [22, 61, 64, 65]. The small reduction of the elongation at the break was noticed from PS/Aero (declining less than 3% compared to the pristine PS) because the exfoliated dispersion of the individual layered clay implied the good interaction between the individually delaminated clay sheets and polymer matrix [61]. On the contrary, the significant drop of the elongation at the break was observed from the nanocomposites prepared using organoclay decreasing by about 18%, 24%, and 29% of PS/ORG-1, PS/ORG-2, and PS/ORG-3, respectively. The results implied that the exfoliated morphology of the nanocomposites has more effect on the reduction of the elongation than the intercalated structure because of the strong interaction between the components of the clay particles and PS matrix [61].

The DSC thermograms of PS/Aero and PS/ORG are presented in Figure 10 and Table 6. The pristine PS revealed an endothermic peak indicating the glass transition temperature (T_g) was about 96.3°C. The significant shift in T_g of PS/Aero to 102–104°C (from 1 to 3 wt.% of the clay loadings) exhibited the improvement of ~6–8°C, compared to that of pure PS. According to the exfoliated dispersion of single nanoclay particles with high aspect ratios in the polymer matrix, the confinement of the PS chains at the organic-inorganic interface clearly resulted in obstructing the segmental motion of the PS chains [13, 61, 64, 65]. Furthermore, the lower T_g values of PS/ORG than PS/Aero are observed in Figure 11 and Table 6. As reported in many studies, the higher increase in T_g was achieved from the exfoliated structure than the intercalated structure of the PS-clay nanocomposites [19, 20, 24, 61, 67–70].

The thermal degradation behavior of the PS-clay nanocomposites was demonstrated in the TGA and DTG thermograms (Figure 11), and the details of the onset decomposition temperature ($T_{d,onset}$), the maximum decomposition rate temperature ($T_{d,max}$), and residual weight at 800°C are reported in Table 6. The decomposition temperatures ($T_{d,onset}$ and $T_{d,max}$) dramatically enhanced the

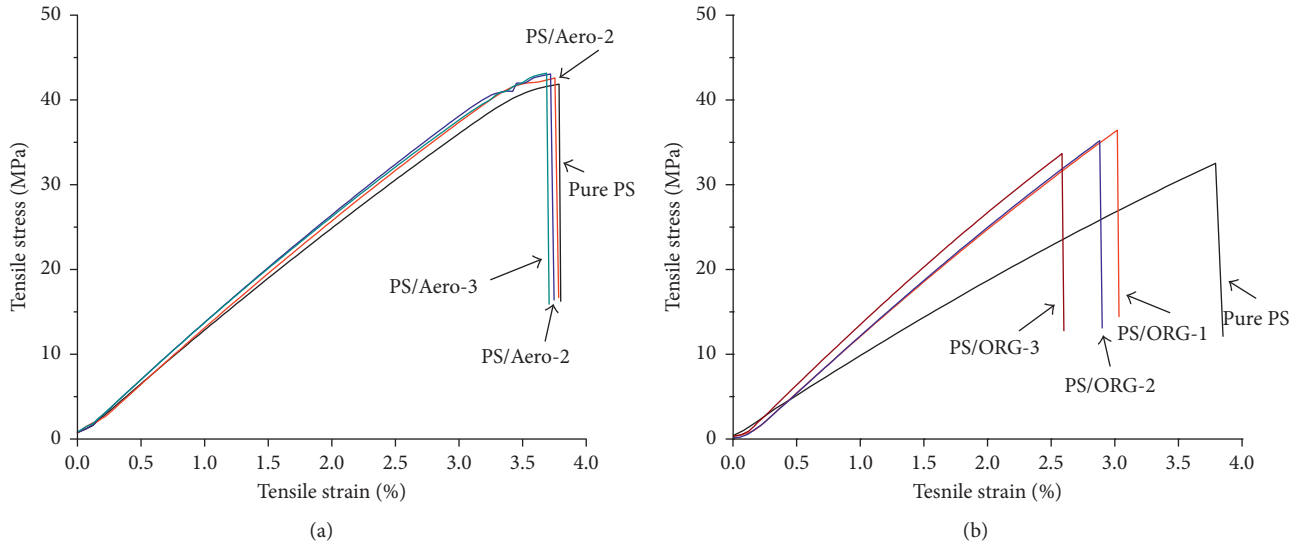

Figure 9: Stress-strain curves of PS/clay nanocomposites prepared from the nanoclay aerogel masterbatch and organoclay.

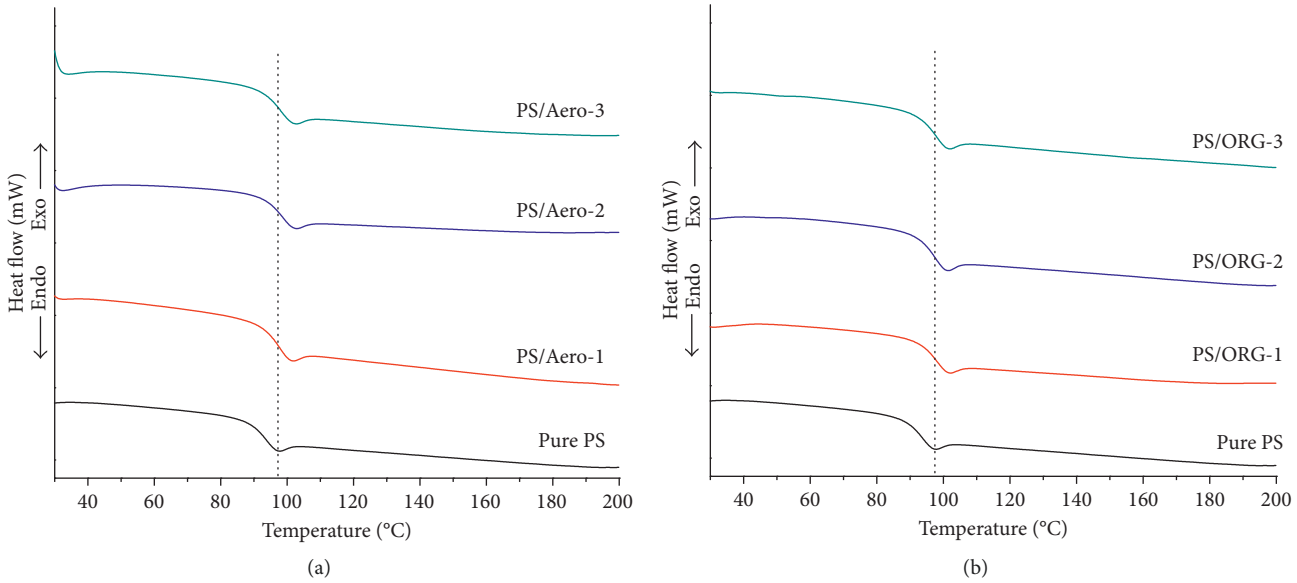

Figure 10: DSC thermograms of PS/clay nanocomposites prepared from the nanoclay aerogel masterbatch and organoclay.

Table 6: DSC and TGA results of PS/clay nanocomposites prepared from the nanoclay aerogel masterbatch and organoclay.

Sample	T_g (°C)	$T_{d,onset}$ (°C)	$T_{d,max}$ (°C)	Residual mass (%)
Pure PS	96	395	422	1
PS/Aero-1	102	418	439	1
PS/Aero-2	104	421	441	2
PS/Aero-3	104	422	443	3
PS/ORG-1	99	410	435	1
PS/ORG-2	99	413	439	2
PS/ORG-3	100	416	440	3

incorporation of nanoclay, and the increment in the degradation temperature was evident with the increase from 1 to 3 wt.% of nanoclay loading. The homogeneous dispersion of nanoclay within the polymer matrix delayed the permeability of the degraded outcomes of the material [17, 19, 25]. The decomposition temperatures of PS/Aero ($T_{d,onset}$ at about 418–422°C and $T_{d,max}$ at about 439–443°C) were higher than those of PS/ORG ($T_{d,onset}$ at 410–416°C and $T_{d,max}$ at 435–440°C) because the exfoliated nanocomposite structure potentially retarded the permeability of the degraded volatiles as compared to the intercalated morphology [71, 72].

4. Conclusions

Attempts have been carried out to obtain the exfoliated-type polymer-clay nanocomposites, but the achieved cases have not yet been found quite often, especially for a system

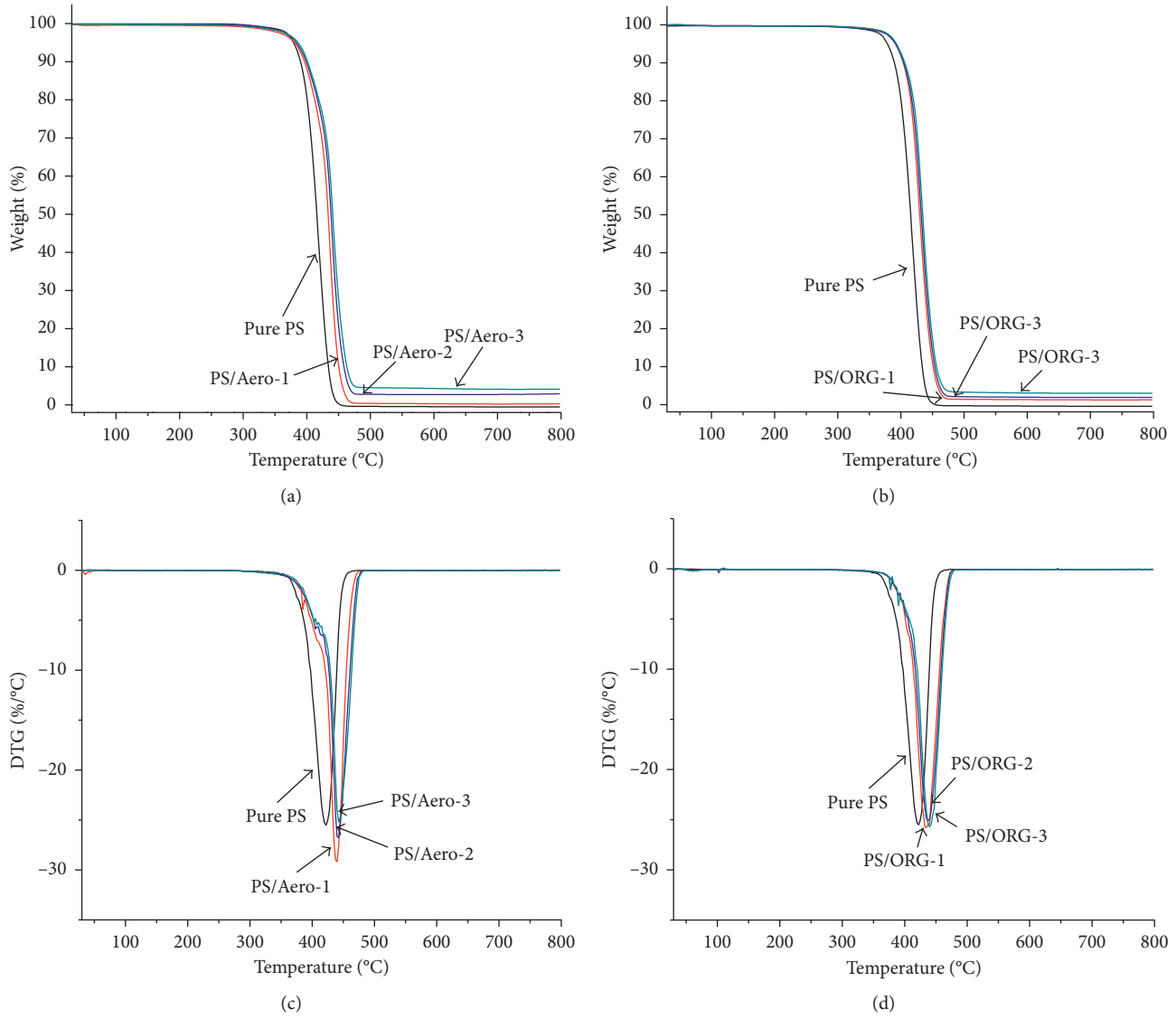

Figure 11: TGA and DTG thermograms of PS/clay nanocomposites prepared from the nanoclay aerogel masterbatch and organoclay.

starting with hydrophobic or nonreactive polymers and pristine clay. In this work, we showed that, without using surfactants like alkylammonium ions to make organic-like clay compatible with organic polymers, the exfoliated polymer-clay nanocomposites could be achieved in a simple and cost-effective procedure. However, this was successfully achieved not only when using 1 wt.% of nanoclay gel (PS/Aerogel-1) but also when using 2 and 3 wt.% nanoclay gels (PS/Aerogel-2 and PS/Aerogel-3) for the system of the opposite polarity and nonreactive (incompatible) components (PS and clay). Moreover, this strategy was prominently due to many advantages, such as the high nanoclay-loading capacity, high layered silicate expansion, high thermal stability, easy handling rather than fine powder, low ingredient and production costs, environmentally friendly process, zero waste, and lean preparation for polymer-clay nanocomposite industries. This result clearly revealed that the mechanism of the pristine clay tactoids exfoliated in the polymeric matrix enhances the mobility of the clay layers. This achievement was carried out in a novel way by attaching the clay layers directly to a mobile polymer, for example, PEG, via hydrogen bonding and ensuring good dispersion of the treated clay layers into a polymer matrix by keeping the PEG-clay intercalated state with a small amount of anionic polymer hydrogel, for example, KC, and turning it to a highly porous and fragile structure by freeze-drying, which is also called a nanoclay aerogel masterbatch. The facile nanoclay aerogel masterbatch was able to be attained even at high clay loadings (55–67 wt.% of the inorganic clay content) with constant PEG and KC loadings. The XRD results exhibited that the PEG molecules were intercalated into the clay galleries to enlarge the interlayer spacing of around 17 Å even at high nanoclay loadings (55–67 wt.%). The SEM micrographs illustrated the typical lamellar morphology, which is also called the house of cards structure. The density values were within 0.108–0.122 g·cm^{-3} and rose with the increased nanoclay loading. The thermal stabilities exhibited up to 270°C of the starting thermal decomposition and up to

340°C of the maximum thermal decomposition, implying these nanoclay aerogel masterbatches were safe to mix with commodity plastics at a high melting temperature. The flowability and processability were certified by the MFI results. Therefore, the highest nanoclay-loading capacity (67 wt.%) of the achieved nanoclay aerogel masterbatch was proper and selected to prepare PS-clay nanocomposites via a melt-mixing process compared to the PS-clay nanocomposite prepared by using organoclay. The results of XRD and TEM exhibited that the exfoliated morphologies were obtained at all clay contents (1–3 wt.%), but on the contrary, the intercalated structure was gained by using organoclay. The presence of brownish specimens was observed by using organoclay due to the degradation of the organic surfactant. The outstanding transparency and brightness were remarked from the specimens prepared by using the nanoclay masterbatch, revealing better thermal stability of the nanoclay masterbatch than the organoclay. The mechanical properties, the glass transition temperature (T_g), and the thermal stability of the PS-clay nanocomposites prepared by using the nanoclay masterbatch had significant enhancement, as compared to the nanocomposites prepared by organoclay.

Data Availability

All of the data (the X-ray diffraction (XRD), scanning electron microscope (SEM), transmission electron microscopy (TEM), thermal behavior (DSC), thermal stability (TGA), density, melt flow index (MFI), compression testing, and tensile testing data) used to support the findings of this study are available from the corresponding author upon request.

Conflicts of Interest

The authors declare that they have no conflicts of interest.

Acknowledgments

The authors are grateful to The 90th Anniversary of Chulalongkorn University Fund (Ratchadaphiseksomphot Endowment Fund) and The Petroleum and Petrochemical College, Chulalongkorn University, Thailand.

References

[1] A. Usuki, "Application 9-development of polymer-clay nanocomposites by dispersion of particles into polymer materials A2-Hosokawa, Masuo," in *Nanoparticle Technology Handbook*, K. Nogi, M. Naito, and T. Yokoyama, Eds., pp. 458–460, Elsevier, Amsterdam, Netherlands, 2nd edition, 2012.

[2] M. Alexandre and P. Dubois, "Polymer-layered silicate nanocomposites: preparation, properties and uses of a new class of materials," *Materials Science and Engineering*, vol. 28, no. 1-2, pp. 1–63, 2000.

[3] B. Lepoittevin, N. Pantoustier, M. Devalckenaere et al., "Polymer/layered silicate nanocomposites by combined intercalative polymerization and melt intercalation: a masterbatch process," *Polymer*, vol. 44, no. 7, pp. 2033–2040, 2003.

[4] A. Tcherbi-Narteh, M. V. Hosur, E. Triggs, and S. Jelaani, "Effects of surface treatments of montmorillonite nanoclay on cure behavior of diglycidyl ether of bisphenol A epoxy resin," *Journal of Nanoscience*, vol. 2013, Article ID 864141, 12 pages, 2013.

[5] C. Chen and T. B. Tolle, "Fully exfoliated layered silicate epoxy nanocomposites," *Journal of Polymer Science Part B*, vol. 42, no. 21, pp. 3981–3986, 2004.

[6] F. Bergaya and G. Lagaly, "Chapter 1-general introduction: clays, clay minerals, and clay science," in *Developments in Clay Science*, B. Faïza and L. Gerhard, Eds., pp. 1–19, Elsevier, New York City, NY, USA, 2013.

[7] J. F. Wagner, "Chapter 9-mechanical properties of clays and clay minerals," in *Developments in Clay Science*, B. Faïza and L. Gerhard, Eds., pp. 347–381, Elsevier, New York City, NY, USA, 2013.

[8] S. Longo, M. Mauro, C. Daniel, M. Galimberti, and G. Guerra, "Clay exfoliation and polymer/clay aerogels by supercritical carbon dioxide," *Frontiers in Chemistry*, vol. 1, p. 28, 2013.

[9] M.-A. Paul, M. Alexandre, P. Degée, C. Calberg, R. Jérôme, and P. Dubois, "Exfoliated polylactide/clay nanocomposites by in-situ coordination–insertion polymerization," *Macromolecular Rapid Communications*, vol. 24, no. 9, pp. 561–566, 2003.

[10] S. Y. Lee and S. J. Kim, "Expansion characteristics of organoclay as a precursor to nanocomposites," *Colloids and Surfaces A: Physicochemical and Engineering Aspects*, vol. 211, no. 1, pp. 19–26, 2002.

[11] X. Kornmann, L. A. Berglund, R. Thomann, R. Mulhaupt, and J. Finter, "High performance epoxy-layered silicate nanocomposites," *Polymer Engineering and Science*, vol. 42, no. 9, pp. 1815–1826, 2002.

[12] C.-W. Chiu, T.-K. Huang, Y.-C. Wang, B. G. Alamani, and J.-J. Lin, "Intercalation strategies in clay/polymer hybrids," *Progress in Polymer Science*, vol. 39, no. 3, pp. 443–485, 2014.

[13] Rao and J. M. Pochan, "Mechanics of polymer–clay nanocomposites," *Macromolecules*, vol. 40, no. 2, pp. 290–296, 2007.

[14] A. Chafidz, M. A.-H. Ali, and R. Elleithy, "Morphological, thermal, rheological, and mechanical properties of polypropylene-nanoclay composites prepared from masterbatch in a twin screw extruder," *Journal of Materials Science*, vol. 46, no. 18, pp. 6075–6086, 2011.

[15] M. Pannirselvan, A. Genovese, M. C. Jollands, S. N. Bhattacharya, and R. A. Shanks, "Oxygen barrier property of polypropylene-polyether treated clay nanocomposite," *Express Polymer Letters*, vol. 3, no. 6, pp. 429–439, 2008.

[16] E. P. Giannelis, "Polymer layered silicate nanocomposites," *Advanced Materials*, vol. 8, no. 1, pp. 29–35, 1996.

[17] S. Sinha Ray and M. Okamoto, "Polymer/layered silicate nanocomposites: a review from preparation to processing," *Progress in Polymer Science*, vol. 28, no. 11, pp. 1539–1641, 2003.

[18] N. B. Sati, R. K. Musa, and K. G. Rahul, "Polymeric nanocomposites," in *Polymeric Nanocomposites*, pp. 1–13, Carl Hanser Verlag GmbH and Co. KG, Munich, Germany, 2007.

[19] P. Uthirakumar, K. S. Nahm, Y. B. Hahn, and Y.-S. Lee, "Preparation of polystyrene/montmorillonite nanocomposites using a new radical initiator-montmorillonite hybrid via in situ intercalative polymerization," *European Polymer Journal*, vol. 40, no. 11, pp. 2437–2444, 2004.

[20] Y. Li and H. Ishida, "A study of morphology and intercalation kinetics of polystyrene–organoclay nanocomposites," *Macromolecules*, vol. 38, no. 15, pp. 6513–6519, 2005.

[21] W. Xu, Q. Zeng, and A. Yu, "Young's modulus of effective clay clusters in polymer nanocomposites," *Polymer*, vol. 53, no. 17, pp. 3735–3740, 2012.

[22] C. I. Park, W. M. Choi, M. H. Kim, and O. O. Park, "Thermal and mechanical properties of syndiotactic polystyrene/organoclay nanocomposites with different microstructures," *Journal of Polymer Science Part B: Polymer Physics*, vol. 42, no. 9, pp. 1685–1693, 2004.

[23] Q. T. Nguyen and D. G. Baird, "Preparation of polymer–clay nanocomposites and their properties," *Advances in Polymer Technology*, vol. 25, no. 4, pp. 270–285, 2006.

[24] M. Y. Gelfer, H. H. Song, L. Liu et al., "Effects of organoclays on morphology and thermal and rheological properties of polystyrene and poly(methyl methacrylate) blends," *Journal of Polymer Science Part B: Polymer Physics*, vol. 41, no. 1, pp. 44–54, 2003.

[25] X. Fu and S. Qutubuddin, "Polymer–clay nanocomposites: exfoliation of organophilic montmorillonite nanolayers in polystyrene," *Polymer*, vol. 42, no. 2, pp. 807–813, 2001.

[26] A. I. Alateyah, H. N. Dhakal, and Z. Y. Zhang, "Processing, properties, and applications of polymer nanocomposites based on layer silicates: a review," *Advances in Polymer Technology*, vol. 32, no. 4, 2013.

[27] E. Manias, A. Touny, L. Wu, K. Strawhecker, B. Lu, and T. C. Chung, "Polypropylene/montmorillonite nanocomposites. Review of the synthetic routes and materials properties," *Chemistry of Materials*, vol. 13, no. 10, pp. 3516–3523, 2001.

[28] R. C. Mackenzie, "Clay–water relationships," *Nature*, vol. 171, no. 4355, pp. 681–683, 1953.

[29] J. J. Tunney and C. Detellier, "Aluminosilicate nanocomposite materials. Poly(ethylene glycol)–kaolinite intercalates," *Chemistry of Materials*, vol. 8, no. 4, pp. 927–935, 1996.

[30] L. Zampori, P. G. Stampino, C. Cristiani, G. Dotelli, and P. Cazzola, "Synthesis of organoclays using non-ionic surfactants: effect of time, temperature and concentration," *Applied Clay Science*, vol. 48, no. 1-2, pp. 97–102, 2010.

[31] E. Finocchio, I. Baccini, C. Cristiani, G. Dotelli, P. Gallo Stampino, and L. Zampori, "Hybrid organo–inorganic clay with nonionic interlayers. Mid- and near-IR spectroscopic studies," *Journal of Physical Chemistry A*, vol. 115, no. 26, pp. 7484–7493, 2011.

[32] V. Belova, D. V. Andreeva, H. Möhwald, and D. G. Shchukin, "Ultrasonic intercalation of gold nanoparticles into clay matrix in the presence of surface-active materials. Part I: neutral polyethylene glycol," *Journal of Physical Chemistry C*, vol. 113, no. 14, pp. 5381–5389, 2009.

[33] P. Aranda and E. Ruiz-Hitzky, "Poly(ethylene oxide)-silicate intercalation materials," *Chemistry of Materials*, vol. 4, no. 6, pp. 1395–1403, 1992.

[34] E. Ruiz-Hitzky and P. Aranda, "Polymer-salt intercalation complexes in layer silicates," *Advanced Materials*, vol. 2, no. 11, pp. 545–547, 1990.

[35] J. Zhang, S. Wang, D. Zhao et al., "Improved processability and performance of biomedical devices with poly(lactic acid)/poly(ethylene glycol) blends," *Journal of Applied Polymer Science*, vol. 134, no. 33, article 45194, 2017.

[36] K. Campbell, D. Q. M. Craig, and T. McNally, "Poly(ethylene glycol) layered silicate nanocomposites for retarded drug release prepared by hot-melt extrusion," *International journal of pharmaceutics*, vol. 363, no. 1-2, pp. 126–131, 2008.

[37] G. H. Therkelsen, "Chapter 7-carrageenan∗," in *Industrial Gums*, pp. 145–180, Academic Press, London, UK, 3rd edition, 1993.

[38] M. Tako, "The principle of polysaccharide gels," *Advances in Bioscience and Biotechnology*, vol. 6, no. 1, pp. 22–36, 2015.

[39] S. R. Derkach, S. O. Ilyin, A. A. Maklakova, V. G. Kulichikhin, and A. Y. Malkin, "The rheology of gelatin hydrogels modified by κ-carrageenan," *LWT-Food Science and Technology*, vol. 63, no. 1, pp. 612–619, 2015.

[40] J.-W. Rhim, "Physical-mechanical properties of agar/κ-carrageenan blend film and derived clay nanocomposite film," *Journal of Food Science*, vol. 77, no. 12, pp. N66–N73, 2012.

[41] S. Shojaee-Aliabadi, M. A. Mohammadifar, H. Hosseini et al., "Characterization of nanobiocomposite kappa-carrageenan film with *Zataria multiflora* essential oil and nanoclay," *International Journal of Biological Macromolecules*, vol. 69, pp. 282–289, 2014.

[42] W. Wu, K. Wang, and M.-S. Zhan, "Preparation and performance of polyimide-reinforced clay aerogel composites," *Industrial and Engineering Chemistry Research*, vol. 51, no. 39, pp. 12821–12826, 2012.

[43] O. A. Madyan, M. Fan, L. Feo, and D. Hui, "Physical properties of clay aerogel composites: an overview," *Composites Part B: Engineering*, vol. 102, pp. 29–37, 2016.

[44] C. Liu, S. Ye, and J. Feng, "Promoting the dispersion of graphene and crystallization of poly(lactic acid) with a freezing-dried graphene/PEG masterbatch," *Composites Science and Technology*, vol. 144, pp. 215–222, 2017.

[45] J. L. Bonczek, W. G. Harris, and P. Nkedi-Kizza, "Monolayer to bilayer transitional arrangements of hexadecyltrimetylammonium cations on Na-montmorillonite," *Clays and Clay Minerals*, vol. 50, no. 1, pp. 11–17, 2002.

[46] S. M. Alhassan, S. Qutubuddin, and D. Schiraldi, "Influence of electrolyte and polymer loadings on mechanical properties of clay aerogels," *Langmuir*, vol. 26, no. 14, pp. 12198–12202, 2010.

[47] B. K. G. Theng, "Chapter 3-uncharged (nonionic) polymers," in *Developments in Clay Science*, B. K. G. Theng, Ed., pp. 79–110, Elsevier, New York City, NY, USA, 2012.

[48] E. J. M. Hensen and B. Smit, "Why clays swell," *Journal of Physical Chemistry B*, vol. 106, no. 49, pp. 12664–12667, 2002.

[49] B. Chen and J. R. G. Evans, "On the thermodynamic driving force for polymer intercalation in smectite clays," *Philosophical Magazine*, vol. 85, no. 14, pp. 1519–1538, 2005.

[50] F. Clegg, C. Breen, and Khairuddin, "Synergistic and competitive aspects of the adsorption of poly(ethylene glycol) and poly(vinyl alcohol) onto Na-bentonite," *Journal of Physical Chemistry B*, vol. 118, no. 46, pp. 13268–13278, 2014.

[51] L. S. Somlai, S. A. Bandi, D. A. Schiraldi, and L. J. Mathias, "Facile processing of clays into organically-modified aerogels," *AIChE Journal*, vol. 52, no. 3, pp. 1162–1168, 2006.

[52] S. Bandi, M. Bell, and D. A. Schiraldi, "Temperature-responsive clay aerogel–polymer composites," *Macromolecules*, vol. 38, no. 22, pp. 9216–9220, 2005.

[53] T. Wang, H. Sun, J. Long, Y.-Z. Wang, and D. Schiraldi, "Biobased poly(furfuryl alcohol)/clay aerogel composite prepared by a freeze-drying process," *ACS Sustainable Chemistry and Engineering*, vol. 4, no. 5, pp. 2601–2605, 2016.

[54] O. A. Madyan and M. Fan, "Temperature induced nature and behaviour of clay-PVA colloidal suspension and its aerogel composites," *Colloids and Surfaces A: Physicochemical and Engineering Aspects*, vol. 529, pp. 495–502, 2017.

[55] P. Huang and M. Fan, "Development of facture free clay-based aerogel: formulation and architectural mechanisms," *Composites Part B: Engineering*, vol. 91, pp. 169–175, 2016.
[56] T. Pojanavaraphan, R. Magaraphan, B.-S. Chiou, and D. A. Schiraldi, "Development of biodegradable foamlike materials based on casein and sodium montmorillonite clay," *Biomacromolecules*, vol. 11, no. 10, pp. 2640–2646, 2010.
[57] M. D. Gawryla, L. Liu, J. C. Grunlan, and D. A. Schiraldi, "pH tailoring electrical and mechanical behavior of polymer–clay–nanotube aerogels," *Macromolecular Rapid Communications*, vol. 30, no. 19, pp. 1669–1673, 2009.
[58] L. Wang, M. Sánchez-Soto, and T. Abt, "Properties of bio-based gum Arabic/clay aerogels," *Industrial Crops and Products*, vol. 91, pp. 15–21, 2016.
[59] L. Wang, M. Sánchez-Soto, and M. L. Maspoch, "Polymer/clay aerogel composites with flame retardant agents: mechanical, thermal and fire behavior," *Materials and Design*, vol. 52, pp. 609–614, 2013.
[60] L. W. McKeen, "1-Introduction to plastics, polymers, and their properties," in *The Effect of Temperature and other Factors on Plastics and Elastomers*, pp. 1–45, William Andrew Publishing, Oxford, UK, 3rd edition, 2014.
[61] D. J. Carastan and N. R. Demarquette, "Polystyrene/clay nanocomposites," *International Materials Reviews*, vol. 52, no. 6, pp. 345–380, 2007.
[62] U. N. Ratnayake, D. E. Prematunga, C. Peiris, V. Karunaratne, and G. A. J. Amaratunga, "Effect of polyethylene glycol-intercalated organoclay on vulcanization characteristics and reinforcement of natural rubber nanocomposites," *Journal of Elastomers and Plastics*, vol. 48, no. 8, pp. 711–727, 2015.
[63] P. H. C. Camargo, K. G. Satyanarayana, and F. Wypych, "Nanocomposites: synthesis, structure, properties and new application opportunities," *Materials Research*, vol. 12, no. 1, pp. 1–39, 2009.
[64] P. Uthirakumar, M.-K. Song, C. Nah, and Y.-S. Lee, "Preparation and characterization of exfoliated polystyrene/clay nanocomposites using a cationic radical initiator-MMT hybrid," *European Polymer Journal*, vol. 41, no. 2, pp. 211–217, 2005.
[65] S. Mohanty and S. K. Nayak, "Melt blended polystyrene/layered silicate nanocomposites: effect of clay modification on the mechanical, thermal, morphological and viscoelastic behavior," *Journal of Thermoplastic Composite Materials*, vol. 20, no. 2, pp. 175–193, 2007.
[66] S. Su, D. D. Jiang, and C. A. Wilkie, "Study on the thermal stability of polystyryl surfactants and their modified clay nanocomposites," *Polymer Degradation and Stability*, vol. 84, no. 2, pp. 269–277, 2004.
[67] J. Zhao, A. B. Morgan, and J. D. Harris, "Rheological characterization of polystyrene–clay nanocomposites to compare the degree of exfoliation and dispersion," *Polymer*, vol. 46, no. 20, pp. 8641–8660, 2005.
[68] D.-R. Yei, S.-W. Kuo, H.-K. Fu, and F.-C. Chang, "Enhanced thermal properties of PS nanocomposites formed from montmorillonite treated with a surfactant/cyclodextrin inclusion complex," *Polymer*, vol. 46, no. 3, pp. 741–750, 2005.
[69] W. A. Zhang, D. Z. Chen, H. Y. Xu, X. F. Shen, and Y. E. Fang, "Influence of four different types of organophilic clay on the morphology and thermal properties of polystyrene/clay nanocomposites prepared by using the γ-ray irradiation technique," *European Polymer Journal*, vol. 39, no. 12, pp. 2323–2328, 2003.
[70] C.-R. Tseng, J.-Y. Wu, H.-Y. Lee, and F.-C. Chang, "Preparation and characterization of polystyrene–clay nanocomposites by free-radical polymerization," *Journal of Applied Polymer Science*, vol. 85, no. 7, pp. 1370–1377, 2002.
[71] H. Li, Y. Yu, and Y. Yang, "Synthesis of exfoliated polystyrene/montmorillonite nanocomposite by emulsion polymerization using a zwitterion as the clay modifier," *European Polymer Journal*, vol. 41, no. 9, pp. 2016–2022, 2005.
[72] J. Zhu, A. B. Morgan, F. J. Lamelas, and C. A. Wilkie, "Fire properties of polystyrene–clay nanocomposites," *Chemistry of Materials*, vol. 13, no. 10, pp. 3774–3780, 2001.